

POLARIMETRIC DECOMPOSITION ANALYSIS OF ALOS-2 PALSAR FOR WETLAND LANDSCAPE AFFECTED BY WILDFIRE NEAR MARGARET LAKE, ALBERTA

PI No:xxxxxxx

Bob Stankovic¹, Ridha Touzi², Jinkai Zhang¹

¹ Wildfire Management Branch, Alberta Agriculture and Forestry

² Canada Centre for Mapping and Earth Observation, Natural Resources Canada

ABSTRACT

This paper describes the use of full polarimetric ALOS2 data to supplement ground cover classification based on optical data in province of Alberta. We utilize multi-temporal SAR data to map non-treed fens. In this paper, we use several forms of polarimetric analysis and decomposition. All of these indicate that the backscatter from graminoid fens in Northern Alberta is dominated by polarimetric characteristics normally attributed to the odd-bounce mechanism and double bounce. For the same wavelength or incidence angle, the ratio of backscatter from the flooded forest to that from the upland forest was higher at HH polarization than at VV polarization. HH+VV backscatter is relatively strong and discrimination between bogs and fens seems to be viable during October month, when the backscatter separation between these two wetland types widens (figure 6). Amount of double bounce scattering is variable throughout the season and the peak is in November's image. The fully polarimetric data have role to play in enhanced ground cover classification which could most certainly improve Alberta forest fuel classification.

Keywords: wetland, polarimetry, incidence angle, backscatter

1. BACKGROUND

Looking at what grows in the northern boreal wetland can also give one a clue to whether it is a bog or a fen. In a northern boreal bog, you can expect to find Black spruce (*Picea Mariana*), Labrador Tea, Cloudberry, Leatherleaf, and Sphagnum moss. In a northern boreal fen, one may also find black spruce, as well as White Spruce (*Picea glauca*), but also expect to find Tamarack (*Larix laricina*), willows, sedges and fen mosses. Often referred to as muskeg, bogs and fens provide important ecosystem services. Bogs store and release water to and from the surrounding land, but are not connected to a system of lakes or streams. Bogs are nutrient poor and generally have low plant diversity as a result. Fens, on the other hand, are connected to slow, but flowing water of small lakes and streams. Both fen and bog are characterized by peat and poorly decomposed vegetation. In fens water level is close to the surface (within 10 cm), while in bog is

below 30 cm [14]. Unlike Tamarack, Black Spruce in a bog enables forest fire to spread easily. Separation of these two features is important in regard to wildfire management.

Wetland mapping with SAR imagery depends on the type of wetlands, water levels, vegetation structure, density and height. The incidence angle, which is the angle between the radar beam and the ground surface, can affect the appearance of smooth targets on the image. The influence of incidence angle on backscatter varies according to forest structure (i.e., basal area, canopy height, canopy depth, and branching qualities) and ground layer characteristics, including surface roughness, soil moisture, and the presence/absence of standing water [9]. Furthermore, the incidence angle has significant influence on the backscatter process from flooded vegetation areas. Backscatter is expected to vary with incidence angle in flooded and non-flooded forests, under leaf-on and leaf-off conditions. This has to be considered in classification algorithms, especially when the data are characterized by a large range of incidence angles. SAR imagery has been used for wetland classification alone or in combination with optical data [2] and is particularly useful for mapping flooded vegetation because of the canopy penetration and subsequent interaction with the underlying water surface [9].

Microwave energy transmitted at smaller (steeper) incidence angles takes a shorter route through the canopy, increasing transmissivity in the crown layer and leaving more energy to interact with the trunk and ground layers. Steep incidence angles (20°-30°) are optimal for detection of flooding, since some forest types exhibit bright returns only at steeper angles [9] or are better able to penetrate vegetation, and thus can better detect flooded vegetation [11]. Many studies concluded that smaller incidence angles were preferable for distinguishing flooded from non-flooded forests ([15]. Others have not shown incidence angle to affect the ability of SAR data to detect flooding beneath vegetation [9]. The increased penetration can also enhance the double bounce scattering of flooded forests which then helps map inundated vegetation during flood events or as a function of the seasonal changes in water level.

In contrast, shallower incidence angle signals have a stronger interaction with the canopy. This results in increased volume scattering [3]. Shallow angle data is more suitable for discriminating between different types of upland vegetation surrounding the wetlands and between different wetland vegetation associations like various sedge, grass, and rush communities [3]

In non-flooded forests, increases in soil moisture raise surface backscatter coefficient and multi-path scattering. However, the increase in double bounce and multi-path scattering that flooding causes is much higher than the increase caused by higher soil moisture levels (1). Increases in canopy foliage leaf area index (LAI) during the warmer months decrease the transmissivity of the crown layer and thus decrease the amount of microwave energy reaching the forest floor. Therefore, an increase in foliage should reduce the ability to detect flooded forests using SAR data, because at larger (shallower) incidence angles signal interacts more with the canopy. Thus decreased transmissivity in the crown layer increases the ability of the radar to estimate canopy characteristics (10). Studies employing multi-polarized data indicate advantages of like-polarization (HH or VV) for the separation of flooded and non-flooded forests [12]. According to [1], the backscatter ratio between flooded and non-flooded forest is higher at HH polarization than at VV polarization.

2. OBJECTIVES

In wildfire management it is critically important to have accurate fuel type maps. The overall objective is to characterize the wetland areas in more accurate manner while combining SAR and optical remote sensing data products. First objective is to gain an understanding of the backscattering characteristics of flooded and non-flooded habitats. One of the objectives of this paper is to determine the influence of incidence angle on the ability of SAR data to detect flooding under forest.

3. STUDY AREA

Margaret Lake site is located in wildfire prone landscape dominated by Black Spruce (*Picea Mariana*) bogs and fens. The drainage is poor or inundated. Frequent wildfires make land cover mapping even more complex. In reality it is a Boreal Forest and this project area overlaps with four natural sub regions: Dry Mixedwood, Sub-Arctic, Boreal Highlands (Caribou slope) and Wetland Mixedwood. The area is located 40 kilometers (25 miles) east of the town of High Level in the Alberta province of Canada

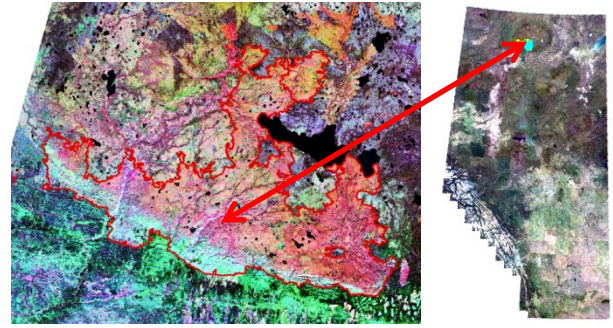


Fig. 1 study area

4. GROUND AND AERIAL DATA

Training data for image classification were gathered in summer 2015 during a ground survey. Several sampling areas were established and on each 3 plots were located and on each plot we collected data such as vegetation species composition, the ground water level and organic matter depth.

Table 1. Alos-2 scenes parameters.

Scene identifier	line spacing	pixel spacing	Incidence angle scene at the center
150618	2.773	2.861	27.813
150804	2.784	2.861	36.537
150818	2.784	2.861	36.533
150827	2.773	2.861	27.813
150910	2.773	2.861	27.815
150915	2.784	2.861	36.533
150929	2.784	2.861	36.532
151008	2.773	2.861	27.806
151022	2.773	2.861	27.806
151105	2.773	2.861	27.806

The Government of Alberta (GOA) has received a multi temporal set of Alos-2 Palsar data in 2016 from JAXA (*Japan Aerospace Exploration Agency*). SLC format PALSAR Full-polarimetry images (Table 1) that have been used for the study area were in Level 1.1 geo-coded format. Pixel Spacing is the distance between adjacent pixels and is measured in metres. This is the same as the pixel size. The pixel spacing may be different for range and azimuth. Nine ALOS-2 scenes were processed for the analyses. For processing work we utilized SNAP and PWS softwares which were made freely available by European Space Agency (ESA) and Natural Resources Canada respectively.

5. APPROACH

A major problem in analyzing polarimetry SAR data is in understanding the scattering mechanisms that makes certain features stand out in the different polarization parameters. To have an RGB image as a reference in analysis, we created calibrated and Lee filtered each polarization band and placed “HH + VV” ,”HV” and “HH – VV” into blue-green-red guns. These combinations are sensitive to different scattering mechanisms. “HH + VV“ is sensitive to single bounce, “HH – VV “ is sensitive to double bounce and “HV” to volumetric and random scattering. Depolarization of a signal causes high return in a cross pol band which tends to be green in areas of denser and taller vegetation. The resulting RGB image (fig 4) shows surface scattering in blue, double bounces are shown in red and volume scattering in green. This result is consistent with the canopy backscatter theory that the HV backscatter comes predominantly from tree crown scattering. The figure 4 depicts a graminoid fen which is dominated by single scattering mechanism which is tall grass in this case. Also double bounce indicated by red color shows another scattering mechanism which in this case is likely water.

The workflow of the data preprocessing is visualized in figure 2. In the first step of processing subsets of all images were created. Then, data were calibrated and saved into a complex format. Calibration radiometrically corrects a SAR image so that the pixel values truly represent the radar backscatter per unit area of the reflecting surface and can be compared with other images.. The data calibration compensates for the radiometric influences of different incidence angles (caused by the sensor geometry and topographic characteristics of the surface).

Since, all the polarimetric tools work with either Coherency or Covariance matrices as input; in the next step we used the matrix generation operator to convert the calibrated complex product into coherency matrices. The reflectivity of the area being observed at a given radar wavelength can be represented by "scattering matrix". Each of the four complex elements of this matrix is the amplitude and phase of the backscattered radiation as measured at one of four orthogonal transmit/receive polarizations. The coherency matrix T3 was preferred because its elements have a physical interpretation (odd-bounce, even-bounce, diffuse, etc.). Most of the targets on the ground are distributed targets and they have mixed scattering responses due to the target properties and the system properties of the Radar beam incident on it.

In the next step , we applied filtering using Refined Lee speckle filter with 7 by 7 window. . Polarimetric speckle filters take advantage of all bands and preserve the complex information at the same time. To interpret this response and separate between different scattering contributors, we applied Freeman-Durden decomposition which was chosen because some studies have demonstrated its ability for mapping flooded vegetation

and wetlands [4]. The Freeman decomposition models the covariance matrix as the contribution of three scattering mechanisms volume scattering (where a canopy scatterer is modeled as a set of randomly oriented dipoles.), double-bounce scattering (modeled by a dihedral corner reflector.) and surface or single-bounce scattering (modeled by a first-order Bragg surface scatterer). Polarimetric SAR decompositions are useful for discriminating and mapping the Earth's surfaces according to scattering behaviors. The Freeman-Durden decomposition was then derived to separate the total power of each pixel into surface, double-bounce, and volume scattering. The output was a three channel image corresponding to the power of each of the three scattering mechanisms. In addition to Freeman decomposition we run Touzy and H- α decomposition as well.

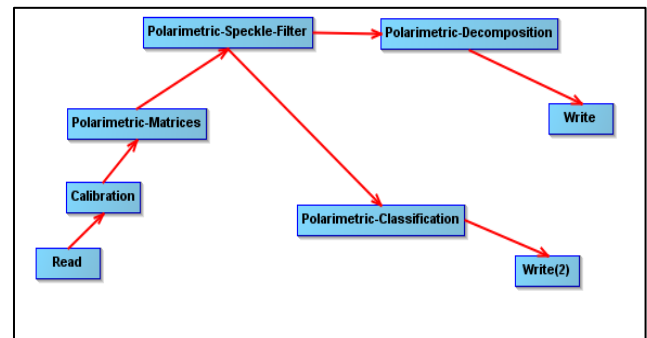


Fig. 2 Methodology to create a classified product

In the final step, Wishart H-alpha Classification was applied to the speckle filtered T3 product to create an unsupervised polarimetric classification and to group similar pixels into classes. This single band contains several regions each belonging to one of nine classes. The classification technique used here is based upon polarimetric decomposition classification parameters-Entropy (H), Anisotropy (A) and Alpha (α). This set of parameters is derived from an eigen value decomposition of the coherency matrix. The entropy provides information on the scattering degree of randomness. The alpha parameter indicates the nature of the scattering: single or double bounce reflection or scattering over anisotropic media. The anisotropy provides information on the relative importance of secondary mechanisms. This parameter cannot be interpreted separately from the entropy. Finally, both the intensity and polarimetric products were corrected to enable us to utilize field data.

Our field data point shape file of field locations was buffered with 20 m radius. These polygons were used as ROI's(regions of interest) to extract individual SAR pixel's intensity values for each polarization and each image. Afterwards, we extracted mean values for all pixels in each polygon and for each polarization and for each image date.

6. RESULTS AND DISCUSSION

In this section, we present the SAR backscatter analysis in the study area. From experience, it was found that wetland boundaries are very difficult to identify using exclusively optical data (Fig.3). Peatland are sphagnum moss with alive spongy material and air in it. Water ascends and descends in peat, and during a year changes in water level may go in range 50 cm up to 1m. Water table may drop but soil moisture and gas bubbles in peat stay. We also measured the same path across the graminoid fen feature with water on the image and the distance in June's image was 916 m and on November's image 848m. Peat rises and goes up and down as water level vary across a season.

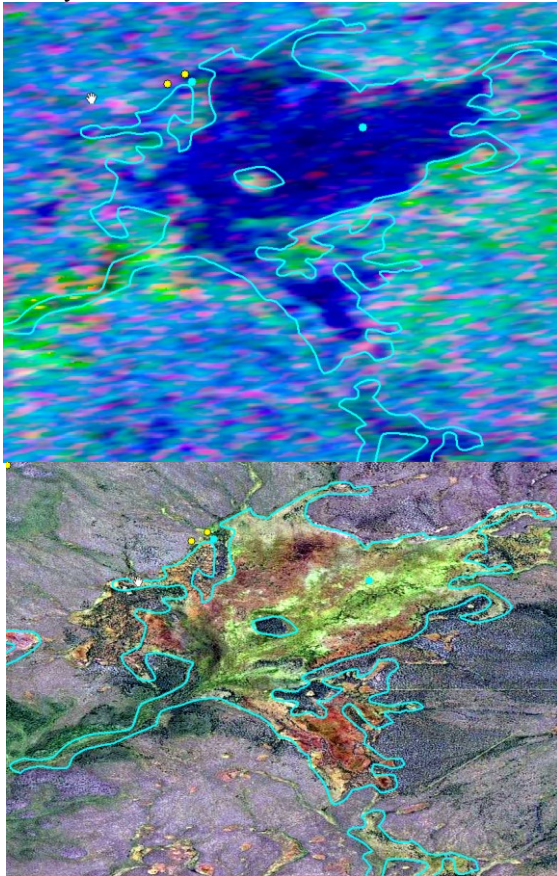


Fig. 3 This graminoid fen is dominated by single bounce. Double bounce is of second importance

In order to gain more understand on the scattering processes of microwave radiation interaction with ground cover, as well as changes in these scattering processes due to inundation, the backscattering values collected using ROI's were compared and analyzed. Original intensity bands were calibrated and filtered using Lee Sigma filter for single image with window size 7 by 7 and sigma 0.9. HH and VV values are similar (Fig. 4) for the open uplands including open white spruce stands and regenerating pine following fire disturbance. White spruce on moist sites with higher moisture have strong signal in

HH. Though variability is greatest in HH polarization and smallest is in HV polarization. Upland sites have a downslope in trend in backscatter from June to beginning of the winter. This finding complies with other studies and it is likely a result in decreasing moisture in plants and soil [2].

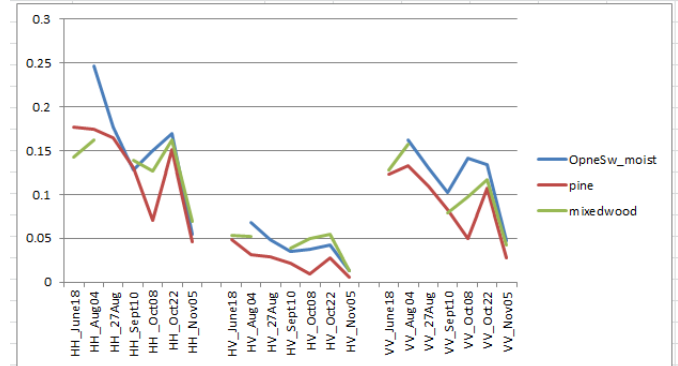


Fig. 4 Alos-2 calibrated and speckle filtered backscatter for HH, HV and VV polarizations.

When it comes to wetland, the finding were similar in these three non-treed fens dominated by water saturated mosses and grasses. These graminoid fens where water level is near the top of soil have cross polarized backscatter significantly low (-20dB) in comparison to the HH and VV components. We noticed that the overall backscatter of these graminoid fens is similar in June and September, but it takes a dive before October ends. This complies with other studies that concluded that many of the land cover types exhibit decreases in backscatter from June to November. This may be attributed to drying conditions due to senescence in the fall [2]. It is unexpected that VV is similar to HH, because it was reported in literature [2] that in marshes and swamps HH is considerably greater than VV. The reason may be that in these fens water level is below the surface and high soil moisture drives signal.

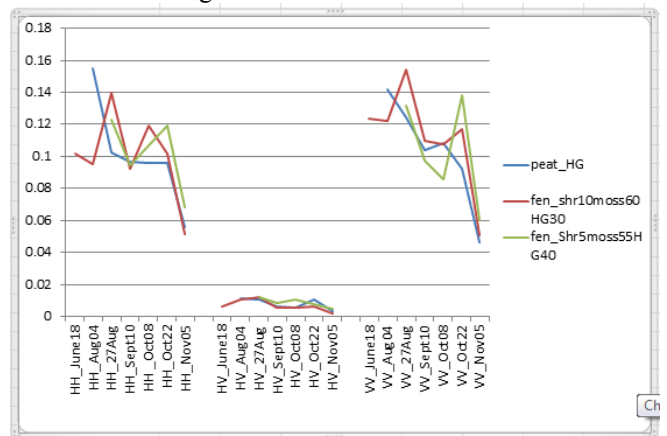


Fig. 5 Alos-2 calibrated and speckle filtered backscatter for HH polarization

It is really important to separate treed fens dominated by Tamarack (*Larix laricina*) from bogs dominated by Black Spruce (*Picea mariana*). When we look at HH+VV backscattering components (figure 6), imagery collected in October may offer more power to discriminate between bogs and fens. In this month the HH+VV combination component creates wider gap between bogs and fens in dB units. Fens backscatter may be stronger than bog's for 1 dB. Similar findings was reported by Henderson in his review stating that HH and VV is preferable to separate between flooded and not flooded forests[5].

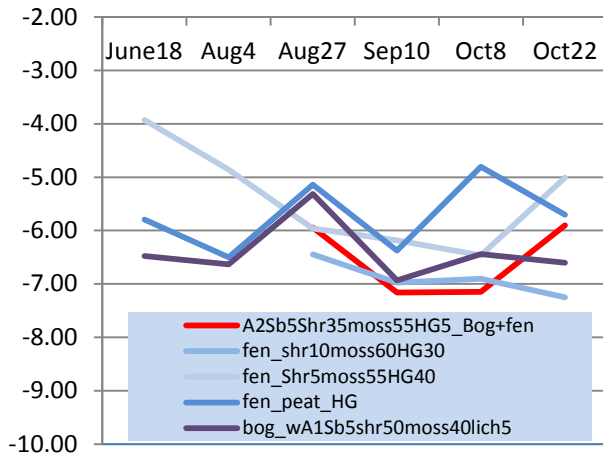


Fig 6. HH+VV backscatter for graminoid fens and bog.

Ratio of flooded and not flooded vegetation

Given the same wavelength or incidence angle we looked at the ratio of backscatter from the graminoid fens to that from the non-flooded forest in this case upland (Open Sw and Pine). For flooded sites we used graminoid fens with water level at the top. Only ratio for HH image from August 4 with incidence angle 36 at the center scene showed -2 dB. The ratio value for four scenes with 28 degrees Incidence angle at the center scene showed range between -1.2 -2.5 dB. Ratio was higher at HH polarization overall than at VV polarization. October 8th SAR scene exhibited the highest variability for both polarizations. Shallow incidence angle (36 degrees) for August 4 image in VV exhibited smallest ratio (0.5 dB). Other studies [1] compared the flooded and nonflooded forests and found that the decrease of the ratio with an increase of incidence angle is a result of the decreased trunk-ground and canopy-ground interactions. The largest backscatter ratio (about 2.5 dB of L band-HH backscatter is modeled at $\theta = 20^\circ$, and the smallest ratio (about 0 dB) at incidence angle = 60° . Like polarization (HH, VV) was deemed preferable to separate flooded from non-flooded forest and produced higher contrast

between swamps and dry forests than cross-polarization[5].

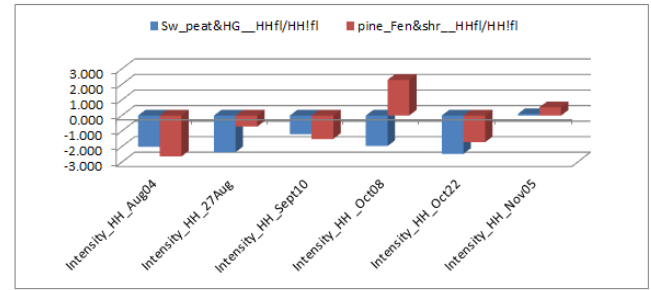


Fig. 6 Ratio flooded vs non flooded for HH polarization and VV ratio below

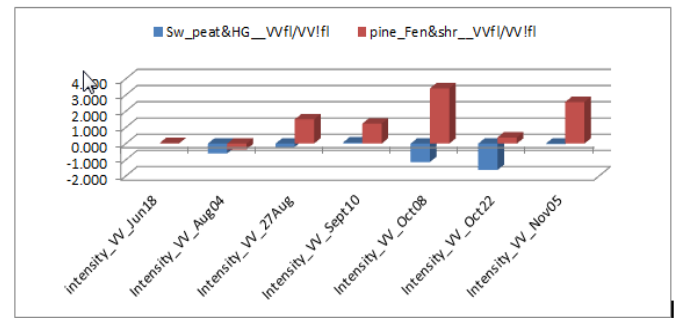


Fig. 7 Ratio of flooded vs none flooded for VV polarization and VV ratio below

HH is best to discriminate between flooded and non-flooded deciduous forests because HH penetrates deeper than HV and VV [11].

Incidence angle effect

When it comes to incidence angles of the SAR imagery, some studies concluded that smaller incidence angles are better able to penetrate vegetation, and thus can better detect flooded vegetation. In this project we utilized imagery with 28° and 36° incidence angle. By visually comparing these images we observed the lower contrast between fens and bogs and increased volumetric scattering component in a 36° image. It seems that volume scattering is getting increased, while surface scattering is getting reduced in the scene with a 36 degree incidence angle (figure 8). Therefore, an increase in foliage should reduce the ability to detect flooded forests using SAR data. In a rather simple exercise we wanted to see if there is any difference in terms of increased volumetric backscatter for different incidence angle. Though, we looked only one site and three images, nevertheless we can report our results that may comply with some studies on this matter conditions [3].

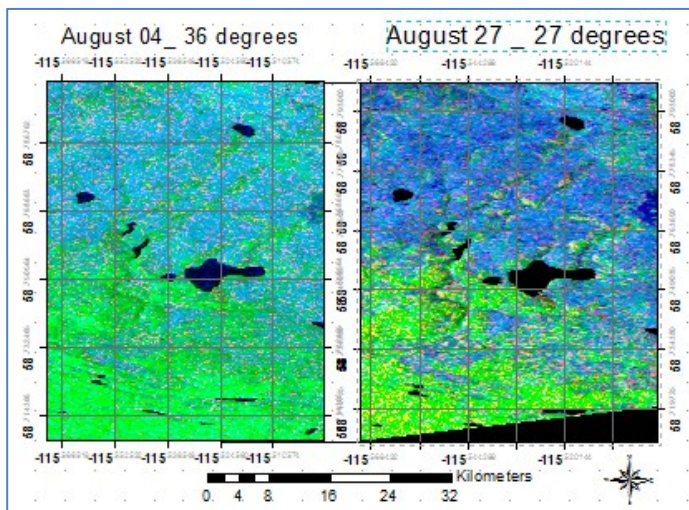


Fig 8 . Two images from August 18 and 27 with different incidence angles

Table 2 HV backscatter for a sample area

Date	8/18/2015	8/27/2015	10/8/2015
Incidence angle	36.53	27.7	2.77
minimum	-23.4	-22.8	-23.9
maximum	0.47	0.8	-0.3
median	-8.4	-9.3	-10.7
mean	-8.3	-9.28	-10.3
variance	3.1	3	3.5
pc75	-6	-7.45	-7.5
pc90	-4.7	-5.8	-5.7

When we compared cross pol (HV) for August 18 (36 °) and August 27 (27 °) for the same spatial area, our statistics showed increased volumetric for image with higher incidence (shallow) angle. Also volumetric

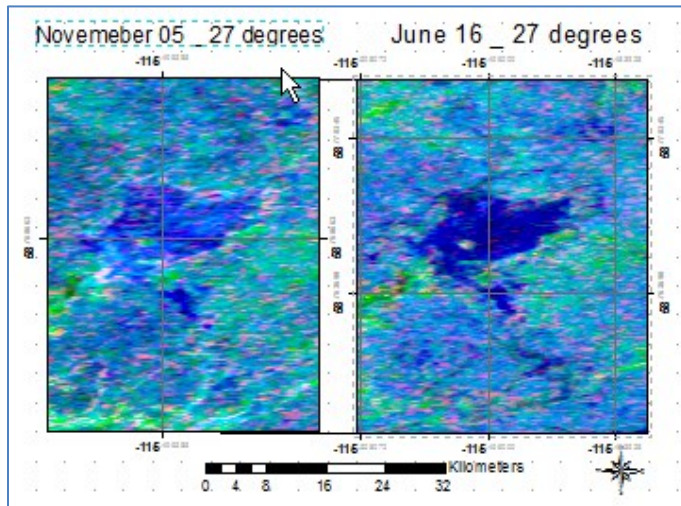


Fig. 9 Freeman Durden decompositions for November and June image

scattering got reduced likely due to less moisture and senescence as the statistics for the October 8 image shows. One limitation here is that in HV we do not account for oriented target scattering. According to literature the large angle diminishes differences between open bog and treed wetland's strong return in VV and HV [11]. Although data collected at average incidence angles of 27.5° and 33.5° were found to provide the best discrimination between flooded and not flooded areas [3]. Studies reported that ability to detect flooding varied more with incidence angle during the leaf-on period and more with forest type during the leaf-off period. During the leaf-on period, canopy transmissivity was primarily responsible for variation in the ability to detect flooding with increasing incidence angle [3].

Double bounce in fen:

Another observation that we noticed was the changes in the amount of double bounce scattering from the fen. through the season. Amount of double bounce is variable throughout the season, but visuallyL the greatest amount of double bounce was visible in November 5 image. Our statistical parameters extracted from Freeman Durden decomposition image shows opposite information (table 3, figure 10). Double bounce has on average stronger signal in June's image than in November, even though surface scattering is less dominant in November image.

Table 3. Differences in scattering mechanisms for November and June

	Freeman_dbl_r	Freeman_vol_g	Freeman_surf_b
18-Jun	-22.950	-14.921	-10.269
5-Nov	-25.684	-16.973	-10.598

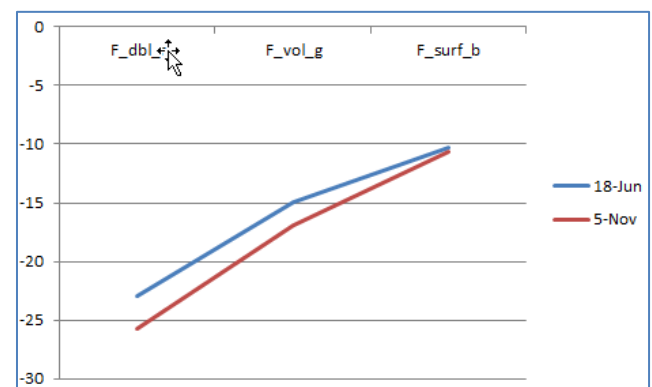


Fig. 10 Differences in scattering mechanisms for November and June

In this case surface scattering remains the constant while double bounce and volume scattering lost some strength by November. Vegetation senescence may play the role in this case. When area is flooded during the leaf-on season, canopy variations among the different forest types were accentuated by increased multi-path and double-bounce scattering which, in turn, increased canopy scattering and

decreased net surface scattering During the leaf-off season(November), when the transmissivity of the crown layer was highest, allowing more energy to penetrate the canopy layer and interact with the surface layer. [3] In this fen, water table drop in summer and as the fall returns water levels once again increase. One could argue that in leaf off conditions double bounce will increase with highly cured vegetation and increased water level.

Classification

Three components can be obtained from the T3 matrix: entropy (H), angle (α) and anisotropy (A). The average α component ranges between 0° and 90° and depends on the dominant scattering mechanism: surface scattering for values near 0° , dipole scattering for values near 45° and double-bounce scattering for values near 90° [16]. High entropy is caused by the depolarizing effects of volume scatter from the structural elements of trees like in pine stands (Table 4), which produce greater disorder in scattering. Alpha is high for forest areas and is low on bare surfaces, snow, and water surfaces. The regions of high entropy can be identified with the help of red colour and low with black colour (Figure 11). Graminoid fen is indicated in Dark colors where entropy is less than 0.4 and is generally a region of low entropy. Bluish zone shows more moderate entropy linked with double bounce. Anisotropy indicator is particularly useful to discriminate scattering mechanisms with different eigenvalue distributions but with similar intermediate entropy values. In such cases, a high anisotropy value indicates two dominant scattering mechanisms with equal probability and a less significant third mechanism, while a low anisotropy value corresponds to a dominant first scattering mechanism and two non-negligible secondary mechanisms with equal importance.

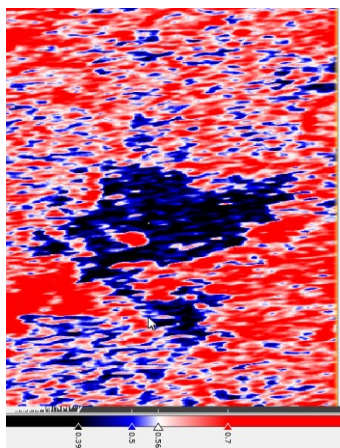


Fig. 11 entropy for the area of a particular fen.

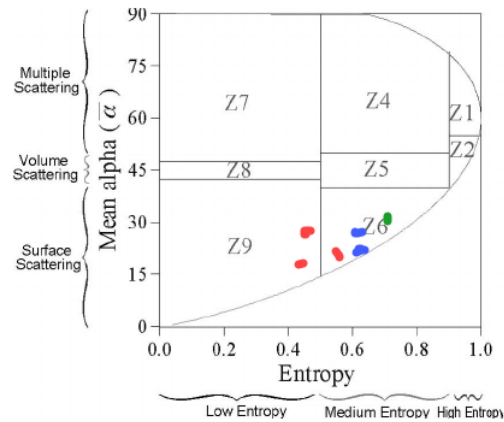


Figure 1. H / Alpha plane. Blue colour indicates bogs, green is for pine and red for fens.

Table 4 H, A, α values for graminoid fen and pine sites

	Sb5Labr75Moss15	fen_moss35gras44	fen_moss60gras44	peat_grass	pine	treed_Sb_bog
Entropy	0.629	0.472	0.458	0.592	0.693	0.635
Anisotropy	0.342	0.257	0.193	0.193	0.293	0.183
Alpha	25.251	17.203	17.067	21.338	30.174	24.311

Surface scattering dominates on these sites including one Lodgepole pine site which has open crown closure. All these sites occupy medium entropy surface scattering corresponding to rough surfaces. Results of the unsupervised segmentation procedure are not presented here. In that work we are implementing phase of the symmetric scattering type [7] and anisotropy.

6..CONCLUSIONS

In this paper, an analysis of multi-temporal Synthetic Aperture Radar data is performed to investigate the general backscatter in an area in Northern Alberta. The focus is on a test area near Margaret Lake. Analyses have shown that the optimum month for separating bogs and graminoid fens is October. Also, imagery with steep angles is preferable over shallow angle. Co-pol polarization (HH, VV) seem to be preferable option to separate flooded from non-flooded forest. During the leaf-on period, canopy transmissivity is reduced and having shallow incidence angle may affect separation of treed wetland from upland. Cloude α angle, entropy and anisotropy should be powerful tools to enable us to detect graminoid fens due to high water ground level. Double bounce signal decreases late in the season, but visually it looks like dominant mechanism comparing to odd bounce. On the other hand graminoid fen in June image visually is dominated by surface scattering, but double bounce is stronger according to measurements.

7. REFERENCES

- [1] Yong Wang, Laura L. Hess, Solange Filoso,* and John M. Melack. Understanding the Radar Backscattering from Flooded and Nonflooded Amazonian Forests: Results from Canopy Backscatter Modeling Remote Sensing of Environment, 1995, vol 54 Issue 3 324-332
- [2] B. Brisco , Frank Ahern et al Polarimetric Decompositions of Temperate Wetlands at C-Band.. IEEE Journal of Selected Topics in Applied Earth Observations and Remote Sensing · July 2015. DOI: 10.1109/JSTARS.2015.2414714
- [3] Megan W. Lang a,, Philip A. Townsend b, Eric S. Kasischke Influence of incidence angle on detecting flooded forests using C-HH synthetic aperture radar data. Remote Sensing of Environment 112 (2008) 3898–3907.
- [4] Lori White, Brian Brisco et al. overview of sar methodologies for monitoring wetlands *Remote Sens.* **2015**, 7(6), 7615-7645; doi:[10.3390/rs70607615](https://doi.org/10.3390/rs70607615) .
- [5] Floyd M. Henderson & [Anthony J. Lewis](#). Radar detection of wetland ecosystems : a review International Journal of Remote Sensing Vol 29. No. 20 .20 October 2008
- [6] <https://sierraclub.bc.ca/a-marsh-a-bog-a-swamp-a-fen/>
- [7] R. Touzi, A. Deschamps, and G. Rother. Wetland characterization using polarimetric RADARSAT-2 capability Can. J. Remote Sensing, Vol. 33, Suppl. 1, pp. S56–S67, 2007
- [8] Eric S. Kasischke Mihai A. Tanase Laura L. Bourgeau-Chavezc Matthew Borra. Soil moisture limitations on monitoring boreal forest regrowth using spaceborne L-band SAR data. Remote Sensing of Environment 115 (2011) 227–232.
- [9] L. L. Hess, J. M. Melack, and D. S. Simonett, “Radar detection of flooding beneath the forest canopy: a review,” Int. J. Remote Sens., vol. 11, no. 7, pp. 1313–1325, Jul. 1990.
- [10] Natalia S. Morandeira 1,2,* , Francisco Grings 2,3, Claudia Facchinetti 4,5 and Patricia Kandus . Mapping Plant Functional Types in Floodplain Wetlands: An Analysis of C-Band Polarimetric SAR Data from RADARSAT-2. Remote Sens. 2016, 8(3), 174;
- [11]. Brigitte Leblon . FOR6304 - Advanced Studies in Radar Polarimetry (RADARSAT 2 –images) at UNB . <http://www.unb.ca/academics/calendar/graduate/current/courses-/fredericton-courses/forestry-courses/index.html>
- [12] S Wu, SA Sader - Multipolarization SAR Data for Surface Feature Delineation and Forest Vegetation Characterization. IEEE Transactions on Geoscience and Remote Sensing. Volume: GE-25 Issue: 1
- [13] F. M. Henderson and A. J. Lewis, “Radar detection of wetland ecosystems: a review,” Int. J. Remote Sens., vol. 29, no. 20, pp. 5809–5835, Oct. 2008
- [14] S.c. Zoltai & D.H. Vitt2 I Forestry Canada, Northern Forestry Centre, Edmonton, Alberta, Canada.
- Canadian wetlands: Environmental gradients and classification . Vegetatio 118: 131-137, 1995.
- [15] L. L. Bourgeau-Chavez ,E. S. Kasischke,S. M. Brunzell,J. P. Mudd,K. B. Smith &A. L. Frick. Analysis of space-borne SAR data for wetland mapping in Virginia riparian ecosystems International Journal of Remote Sensing Volume 22, 2001 - Issue 18 3665-3687
- [16] https://earth.esa.int/documents/653194/.../Polarimetric_SAR_Data_Classification.pdf